

FORMATION OF AROMATIC COMPOUNDS AND SOOT IN FLAMES

R.P. Lindstedt and G. Skevis
 Mechanical Engineering Department,
 Imperial College of Science, Technology and Medicine,
 Exhibition Road, London SW7 2BX, UK.

Keywords: Soot Formation, PAH Formation in Flames, HACA Sequence

ABSTRACT

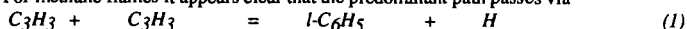
The formation of aromatic compounds such as toluene, naphthalene and phenylacetylene is discussed in the context of soot nucleation in flames. Detailed kinetic reaction steps have been reviewed and a reaction mechanism has been constructed. It is shown that good quantitative agreement between computations and measurements can be obtained for minor aromatic compounds in premixed benzene flames with the notable exception of naphthalene. Benzene flames have been preferred on the grounds that the uncertainties associated with the formation of the first ring can be avoided and as a detailed reaction mechanism for benzene oxidation has recently been proposed. Special attention has been given to species and processes, such as the HACA sequence, which are generally considered essential to the soot nucleation process.

INTRODUCTION

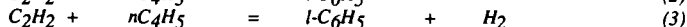
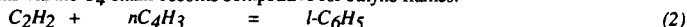
To develop a predictive capability for the formation of PAH and soot in laminar and turbulent flames is of fundamental scientific and practical interest. For diffusion flames with C_1 - C_3 fuels it has been shown [1] that predictions of soot are insensitive to the exact nature of the nucleation process for a wide range of conditions. For example, an *ad hoc* approximation assigning a C_{60} shell as a typical particle size where mass growth becomes dominant over nucleation, has been shown [1] to be satisfactory, provided that nucleation occurs close to the correct location in the flame structure. By contrast, it is reasonable to expect that in premixed flames the dynamics of the nucleation process becomes more important due to shorter time scales. Thus while the use of benzene [1], or even ethyne [2], as indicative species has been shown to be satisfactory in diffusion flame environments, this situation is unlikely to prevail for premixed or partially premixed combustion. Furthermore, many practical fuels, e.g. kerosene, contains a spectrum of aromatic fuel components. Clearly, for these cases current simplified approaches require refinement. The most obvious way of introducing improved descriptions of soot nucleation leads to the introduction of reaction steps for the formation of the second and subsequent aromatic rings. Modelling of the formation of the second ring requires accurate predictions of the underlying flame structure. For benzene flames this has proved difficult in the past. However, recently a benzene oxidation mechanism has been proposed [3] which gives good quantitative agreement for the flame features of relevance to the present study.

CHEMISTRY

Uncertainties have long prevailed regarding the benzene formation steps in flames burning C_1 - C_4 fuels. For methane flames it appears clear that the predominant path passes via

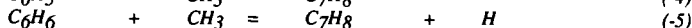
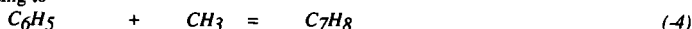


with the subsequent cyclization of the linear C_6H_5 species [3,4]. The situation for higher hydrocarbons is not as firmly established. However, there is some evidence [5] to suggest that reactions via the C_4 chain become competitive for ethyne flames.

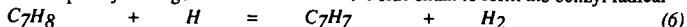


To by-pass the uncertainty associated with the formation reactions for the first ring the present work considers benzene flames. The reaction mechanism used is that proposed by Lindstedt and Skevis [3] which has been shown to predict the MBMS data by Bittner and Howard [6] well.

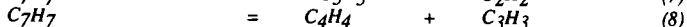
The reaction sequence adopted for toluene, phenyl-acetylene and naphthalene (the second ring) formation is outlined below. Toluene is produced by methyl radical attack on the benzene ring according to



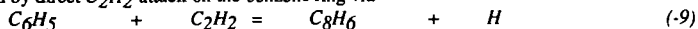
Toluene subsequently undergoes H atom attack on the side chain to form the benzyl radical



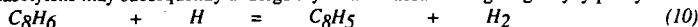
The benzyl radical further dissociates by ring opening either to cyclopentadiene and acetylene or to vinylacetylene and the propargyl radical thus feeding into the C_5 and C_4 chains respectively. Both reactions are assumed to be uni-molecular



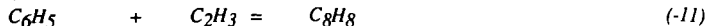
The phenylacetylene mechanism used here is adopted from the work of Herzler and Frank [7] who obtained data in a shock tube at temperatures in the range 1500 - 1900 K. Phenylacetylene is formed by direct C_2H_2 attack on the benzene ring via



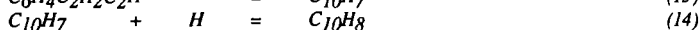
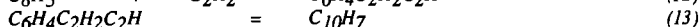
Phenylacetylene may subsequently undergo aryl H atom abstraction giving ethynylphenylene.



Styrene formation was also considered and postulated to occur via vinyl radical attack on the benzene.



The plausibility of naphthalene formation via the building blocks of the *HACA* sequence [8,9] is here investigated further. In the $C_{10}H_8$ formation sequence ethynylphenylene undergoes a further acetylene attack on the free site thus forming a di-substituted aromatic compound which subsequently isomerises to naphthyl radical. Naphthalene is then formed by a second H attack on the ring.



The above mechanism may readily be written in a generalised form for the formation of higher *PAH* [8] and soot. For the latter only the equivalent of reaction (10) is treated as reversible while reactions (12) and (13) are written in a slightly different form. Table 1 provides a listing of the most important reactions and rate coefficients in the present mechanism. The thermodynamic data was mainly obtained from the *CHEMKIN* database [10]. Toluene and naphthalene were assigned ΔH_f values of 12 kcal/mole and 36 kcal/mole respectively, while the heat of formation of the benzyl radical was set at 51.9 kcal/mole. Styrene was assigned a heat of formation of 35.5 kcal/mole. The heats of formation of phenylacetylene, 78.2 kcal/mole, and ethynylphenylene, 133.6 kcal/mole, were adopted from the work of Herzler and Frank [7]. For $C_6H_4C_2H_2C_2H$ the heat of formation was adopted from Frenklach et al [19]. Group additivity [11] was employed to estimate thermodynamic data for species not found in the literature.

RESULTS AND DISCUSSION

The first flame considered in this study was the rich, laminar, low-pressure 21.8% C_6H_6 , 68.2% O_2 , 10% *Ar* flame studied by McKinnon [12]. The flame was assumed to be burner stabilised and the experimental temperature profile was imposed on the calculations. However, it was found necessary to shift the temperature profile by 2 mm with respect to the species concentration profiles in order to account for probe effects. Profiles of the major species are shown in Figures 1 and 2. Clearly, major species are predicted well and the benzene consumption rate is matched. Also the model gives excellent agreement for acetylene and methane concentration levels as shown in Figure 3. The second flame considered was the rich, laminar, near-sooting 13.5% C_6H_6 , 56.5% O_2 , 30% *Ar* flame of Bittner and Howard [6], which has been studied extensively elsewhere [3]. Predictions of toluene and phenylacetylene levels are within a factor of 2 or better as shown in Figure 4. Computations using a lower heat of formation for C_8H_6 - 75.2 kcal/mole as suggested in [10] leads to equally acceptable phenylacetylene levels. Good agreement, again within a factor of 2, was also observed for styrene levels in the flame. Toluene and phenylacetylene profiles are also shown in Figure 5 for the 14.8% C_6H_6 , 55.2% O_2 , 30% *Ar* flame studied by McKinnon [12]. The agreement is again acceptable. Naphthalene chemistry is important because it provides the first step for *PAH* mass growth in flames. Initial computations using the above sequence [8,9] led to severe under-prediction of $C_{10}H_8$ levels - by a factor of 15 or more. In order to partially resolve the issue, the reaction sequence was retained but reactions (12) and (14) were postulated to proceed with a collision efficiency of 5%. This led to an increase of naphthalene levels by a factor of 3, as shown in Figure 6. Even assigning a collision efficiency of 1, unreasonable for a gas phase reaction, results in under-predictions by a factor of 4. Given the accuracy of predictions of other minor aromatic species this is of concern for quantitative predictions of soot nucleation based on the above reaction sequence.

CONCLUSIONS

It has been shown that good agreement between measurements and predictions may be obtained for small aromatic compounds in benzene flames and that consequently improved soot nucleation models may be developed. However, it has also been shown that significant uncertainties surround the reaction sequence for the second aromatic ring. It appears that either the reaction rates in the formation sequence [9] have to be assigned collision efficiencies similar to those used for soot mass growth [8] or that the whole mechanism for second ring formation has to be refined. For gas phase reactions the latter is clearly preferable. This may involve distinguishing between active sites, accounting for steric effects, incorporating attacks by a variety of radicals and exploring supplementary reaction paths.

ACKNOWLEDGEMENT

The Authors Gratefully Acknowledge the Financial Support of British Gas plc.

REFERENCES

- [1] Lindstedt, R.P., in *Mechanisms and Models of Soot Formation* (H. Bockhorn, Ed.), Springer-Verlag, To Appear.
- [2] Leung, K.M., Lindstedt, R.P. and Jones, W.P., *Combustion and Flame* 87, p.289 (1989)
- [3] Lindstedt, R.P. and Skevis, G., Submitted to the *Twenty-Fifth Symposium (International on Combustion)* Nov. 1993
- [4] Leung, K.M. and Lindstedt, R.P., *Comb. and Flame*, To Appear.
- [5] Vovelle, Ch., Delfau, J.-L. and Doute, Ch., *Proc. of Anglo-German Comb. Symp.*, Cambridge 1993, p. 148.
- [6] Bittner, J.D. and Howard, J.B., *Eighteenth Symposium (International) on Combustion*, The Combustion Institute, 1980, p.1105
- [7] Herzler, J. and Frank, P., in *Mechanisms and Models of Soot Formation* (H. Bockhorn, Ed.), Springer-Verlag, To Appear.
- [8] Frenklach, M. and Wang, H., *Twenty-third Symposium (International) on Combustion*, The Combustion Institute, 1990, p.1559
- [9] Frenklach, M. and Warnatz, J., *Comb. Sci. and Tech.* 51:265 (1987)
- [10] Kee, R.J., Rupley, F.M. and Miller, J.A., *The CHEMKIN Thermodynamic Database*, Sandia National Laboratories Report No. SAND87-8215, 1987
- [11] Benson, S.W., *Thermochemical Kinetics*, Wiley, New York, 1976
- [12] McKinnon, J.T., Jr., *Ph.D. Thesis*, Chemical Engineering Department, MIT, 1989
- [13] Miller, J.A. and Melius, C.F., *Combust. Flame.* 91:21 (1992)
- [14] Westmoreland, P.R., Dean, A.M., Howard, J.B. and Longwell, J.P., *J. Phys. Chem.* 93:8171 (1989)
- [15] Emdee, J.L., Brezinsky, K. and Glassman, I., *J. Phys. Chem.* 96:2151 (1992)
- [16] Braun-Unkoff, M., Frank, P. and Just, Th., *Twenty-second Symposium (International) on Combustion*, The Combustion Institute, 1988, p.1053
- [17] Brouwer, L.D., Muller-Markgraf, M. and Troe, J., *J. Phys. Chem.*, 92:4905 (1988)
- [18] Colket III, M.B., Seery, D.J. and Palmer, H.B., *Combust. Flame.*, 75:343 (1989)
- [19] Frenklach, M., Clary, D.W. and Yuan, T., Gardiner, W.C., Jr and Stein, S.E., *Comb. Sci. and Tech.* 50, p. 79 (1986)

Table 1. Reaction Mechanism Rate Coefficients in the Form $k = A T^n \exp(-E_a/RT)$. Units are kmole, cubic metres, seconds, Kelvin and KJ/mole

Reaction	A	n	E _a	Reference
C ₃ H ₃ + C ₃ H ₃ → l-C ₆ H ₅ + H	3.00e10	0.00	0.00	13
l-C ₆ H ₅ → n-C ₄ H ₃ + C ₂ H ₂	1.00e14	0.00	163.72	3
n-C ₄ H ₅ + C ₂ H ₂ → C ₆ H ₆ + H	1.90e04	1.47	20.54	14
C ₇ H ₈ → C ₆ H ₅ + CH ₃	1.14e15	0.00	417.56	15
C ₇ H ₈ + H → C ₆ H ₆ + CH ₃	1.20e10	0.00	21.54	15
C ₇ H ₈ + H → C ₇ H ₇ + H ₂	5.00e11	0.00	52.30	16
C ₇ H ₇ → c-C ₅ H ₅ + C ₂ H ₂	1.66e10	0.00	187.00	17
C ₇ H ₇ → C ₄ H ₄ + C ₃ H ₃	2.00e15	0.00	349.60	17
C ₈ H ₆ + H → C ₆ H ₅ + C ₂ H ₂	2.00e11	0.00	40.58	7
C ₈ H ₆ + H → C ₈ H ₅ + H ₂	4.00e10	0.00	40.58	7
C ₆ H ₅ + C ₂ H ₂ → C ₈ H ₈	5.01e09	0.00	0.00	18
C ₈ H ₅ + C ₂ H ₂ → C ₆ H ₄ C ₂ H ₂ C ₂ H	2.00e11	0.00	0.00	9, pw
C ₆ H ₄ C ₂ H ₂ C ₂ H → C ₁₀ H ₇	1.00e10	0.00	0.00	9
C ₁₀ H ₇ + H → C ₁₀ H ₈	5.00e11	0.00	0.00	9, pw

Figure 1 - Comparison between computed (lines) and experimental (points) profiles for C6H6, H2 and H2O
 Experimental data are from McKinnon [12]

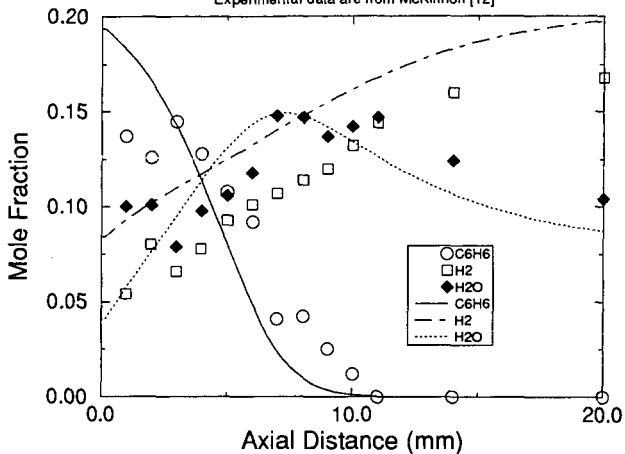


Figure 2 - Comparison between computed (lines) and experimental (points) profiles for O2, CO and CO2
 Experimental data are from McKinnon [12]

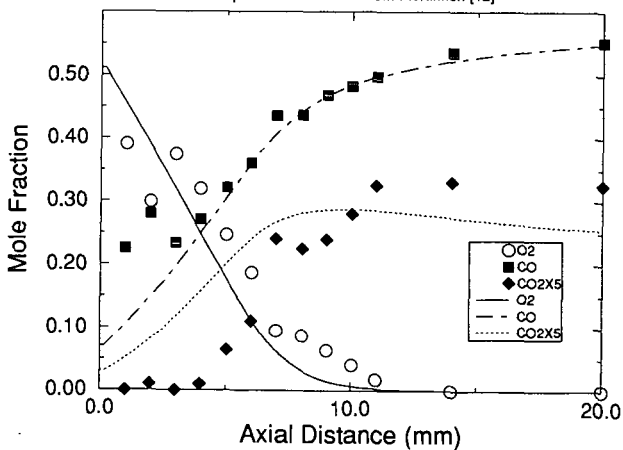


Figure 3 - Comparison between computed (lines) and experimental (points) profiles for C2H2 and CH4
 Experimental data are from McKinnon [12]

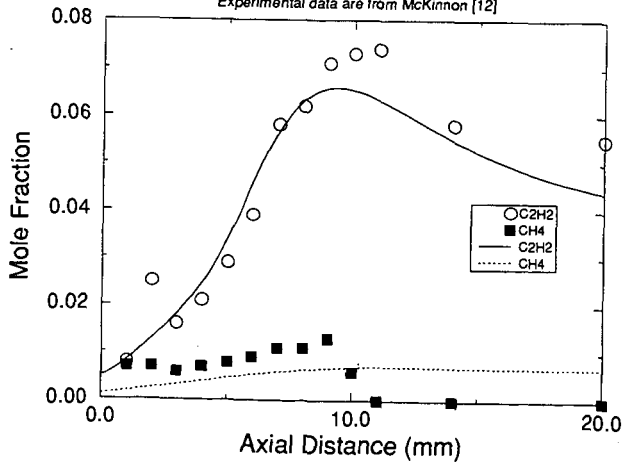


Figure 4 - Comparison between computed (lines) and experimental (points) profiles for C7H8 and C8H6
 Experimental data are from Bittner and Howard [6]

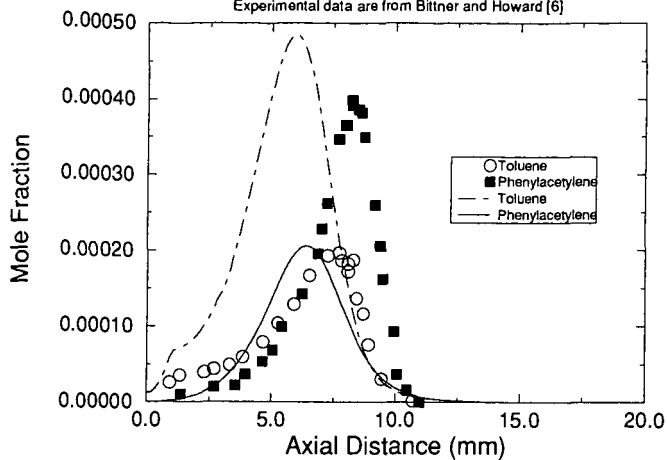


Figure 5 - Comparison between computed (lines) and experimental (points) profiles for C7H8 and C8H6
 Experimental data are from McKinnon [12]

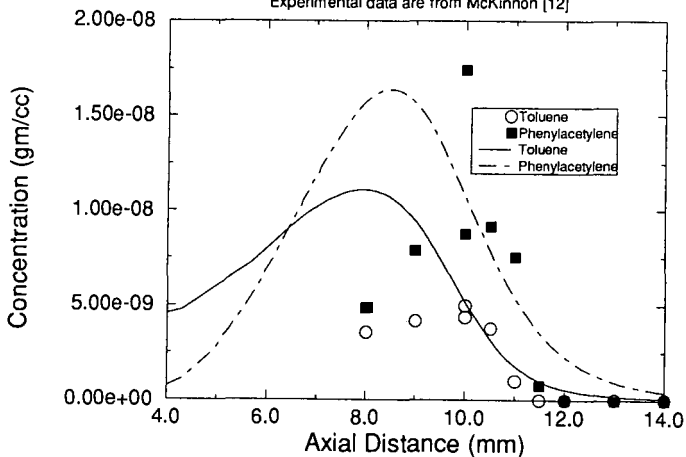


Figure 6 - Comparison between computed (lines) and experimental (points) profiles for C10H8
 Experimental data are from Bittner and Howard [6]

